ON THE ANALYSIS OF SEA SURFACE IMAGES RELATED TO SEA STATE DETERMINATION BY MULTIFRACTAL METHODS (selected from CEMA'19 Conference)

N. Ampilova*, I. Soloviev*, A. Kotopoulis**, G. Pouraimis** and P. Frangos**

* St. Petersburg State University, Comp. Sci. Dept.,

St. Petersburg, Russia

Email: n.ampilova@spbu.ru, i.soloviev@spbu.ru

** School of Electrical and Computer Engineering,

National Technical University of Athens, Greece

Email: pfrangos@central.ntua.gr

Abstract

Digital images may register states of a process, and image analysis help us to study this process and its peculiarities. In spite of the fact that there are a lot of textbooks on techniques of image analysis, any new problem may require a new method. Last decades fractal and multifractal methods are often used to analyze high resolution images having complex textures. In many cases fractal characteristics may be considered as classifying signs for further clustering. In this paper we present two multifractal methods. The first method allows us to obtain multifractal spectra and decompose an initial image into the union of nonintersecting sets. The second one is based on the transformation of an initial measure distribution under so called "direct multifractal transform" and calculation of information dimensions of measure supports. The examples of application of these techniques are given for various kinds of sea surface images.

1. INTRODUCTION

Now the methods of fractal and multifractal analysis are widely used to analyze images with complex structure. Such images are often fractals or multifractals. Fractal sets have a self-similarity property and may be described one numerical characteristic — fractal dimension. Multifractal sets are unions of several fractal subsets, which of them has its own fractal dimension, being these subsets are arranged in a complex intertwined manner. Hence a common characteristic for multifractals is multifractal spectrum — the set of fractal dimensions of its subsets. Our experience in analyzing biomedical preparation images (in [1] we calculated Rényi spectra for images of pharmacological solutions of Ag, and in [2, 3] we applied such methods for sensitive crystallization images) testifies that the good separation of spectra results in successful classification of similar images.

In this work we consider two methods for calculation of multifractal characteristics for digital images: a method based on calculation so called density function, which is calculated for each pixel and characterizes intensity changes in its neighbourhood, and calculation of the set of information dimensions both for a given spectrum and its modified variants which are obtained by a renormalization of a given measure. Additionally, in this method we calculate the spectrum of averaged exponents of singularity. Thus, to characterize an image we have 2 spectra. The combination of two methods increases the possibility for classification of images.

2. MULTIFRACTAL SPECTRUM BY USING DENSITY FUNCTION

We consider a special density function [4] to calculate the singularity power for every pixel. Then we combine all the pixels with close values of density function, which results in partition of the image on the subsets — so called level sets. For each level set we calculate its fractal dimension.

Let μ be a measure defined through pixel intensities for a given digital image. For $x \in R^2$ we denote $B(x,r)$ a square of length r with center x. Let $\mu\big(B(x,r)\big) = kr^{d(x)}(x)$, where $d(x)$ is so called local density function of x, and k some constant. Taking several values for r we have

$$d(x) = \lim_{r\to 0} \frac{\log \mu(B(x,r))}{\log r} \tag{1}$$

The density function measures the non-uniformity of the intensity distribution in the square $B(x,r)$. The set of all points x with local density α is a level set $E_\alpha = \{x \in R^2 : d(x) = \alpha\}$. In practice, not to increase the number of level sets, one really consider the sets $E(\alpha,\varepsilon) = \{x \in R^2 : d(x) \in [\alpha, \alpha + \varepsilon)\}$, where ε is a real number.

The set of fractal dimensions of E_α is the multifractal spectrum $f(\alpha)$.

3. MULTIFRACTAL SPECTRUM BY USING STATISTICAL SUM

It is usually assumed that an image is partitioned by cells with size l, the number of cells is N(l) and the measure of i-th cell is $p_i(l) \sim l^{\alpha_i}$. Consider the statistical sum

$S(q,l) = \sum_{i=1}^{N(l)} p_i^q(l)$) (called also the sum of moments of the measure), where q is a real number, and the sequence of measures $\mu(q,l) = \{\mu_i(q,l)\}$ generated from the initial measure by the direct multifractal transform $\mu_i(q,l) = \frac{p_i^q(l)}{\sum_{i=1}^{N} p_i^q(l)}$. The method proposed in [5] is based on the calculation of information dimension of a measure support M by the formula

$$dim\, M = -\lim_{N\to\infty} \frac{\sum_{i=1}^{N} p_i \ln p_i}{\ln N} \tag{2}$$

The direct multifractal transform recalculates the initial measure by using statistical sum, and hence it depends on q as well. For any measure from the generated sequence one may calculate the singularity power averaged over the measure and the fractal dimension of the support of the measure corresponding to this singularity power. Hence we obtain the averaged singularity spectrum $\alpha(q)$, and the fractal dimension of the support of the measure $f(q)$ as functions of the parameter q. Eliminating q one can obtain the relation between singularity values and fractal dimensions of corresponding subset.

For each measure $\mu(q,l)$ one can calculate information dimension of its support. As q changes, we have a set $f(q)$ of information dimensions of $\mu(q,l)$ supports, where

$$f(q) = \lim_{l\to 0} \frac{\sum_{i=1}^{N} \mu_i(q,l) \ln \mu_i(q,l)}{\ln l} = \lim_{l\to 0} \frac{f(q,l)}{\ln l} \tag{3}$$

We also calculate averaging exponents over the measure $\mu(q,l)$, i.e.

$$\sum_{i=1}^{N} \alpha_i \mu_i(q,l) = \frac{\sum_{i=1}^{N} \ln p_i(l) \mu_i(q,l)}{\ln l} = \frac{\alpha(q,l)}{\ln l} \tag{4}$$

and then the limit $\alpha(q)$ of these averagings when $l \to 0$. Hence, we obtain

$$\alpha(q) = \lim_{l\to 0} \frac{\alpha(q,l)}{\ln l} \tag{5}$$

Such a method allows us to obtain the set of dimensions $f(q)$ and the set of averaging exponents $\alpha(q)$ as functions of the parameter q.

In practice, to obtain the above values we should do the following. For every q we take several values of variable l, calculate sets of points $(\ln l, f(q,l))$ and $(\ln l, \alpha(q,l))$ respectively. Then, by using the least square method, we find the corresponding straight lines (in double logarithmic scale), and their tangent coefficients give us the approximate values of $f(q)$ and $\alpha(q)$ respectively. Thus, we have the set of information dimensions of the supports of the measures obtained from the initial measure by the direct multifractal transform. In [6] we applied this method to analyze biomedical preparation images, and in [7] it was used to study crystallization images.

4. NUMERICAL EXPERIMENTS

4.1 Density function method - Grayscale

Fig. 1. Optical images of sea surface related to sea state determination: calm sea surface (left) and disturbed sea surface (right).

Values of density function lie in diapason $[1.73, 2.23]$ for calm, and $[1.52, 2.42]$ for disturbed sea. We note that wider interval corresponds to more complex structure of the image. Level sets were constructed with step 0.1. The graphs of multifractal spectra are given in Fig. 2, below.

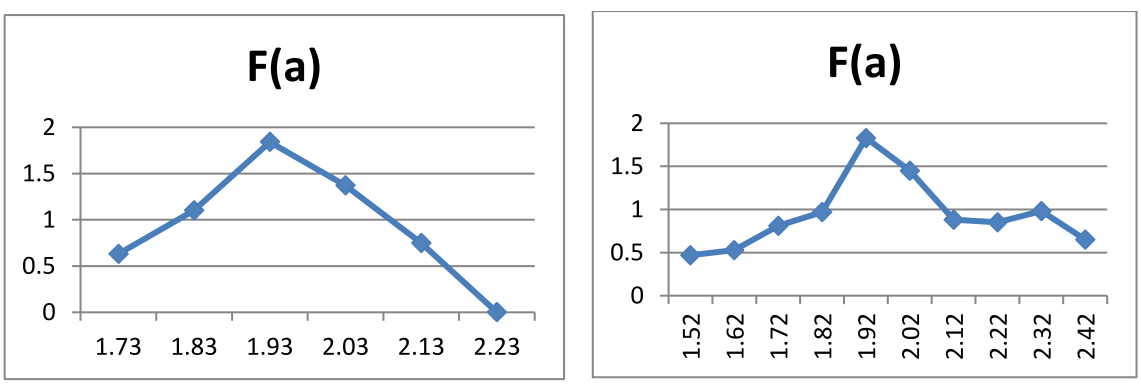

Fig. 2. Multifractal spectrum for calm sea surface (left) and disturbed sea surface (right). The images are represented in grayscale.

Level sets for image of calm sea are shown in Fig. 3, below. These sets illustrate a decomposition of an image on nonintersecting subsets. Each subset contains pixels having density function value in an interval $[a, a + 0.1)$, where $a = 1.73, 1.83, 193, 2.03, 2.13$.

Thus, the number of subsets shown equals the number of intervals between values of $d(x)$ on OX axis. The corresponding graph shows values of fractal dimensions of these sets. We see that image (c) has the most intensive density, and on the graph we see that this subset has the maximal fractal dimension.

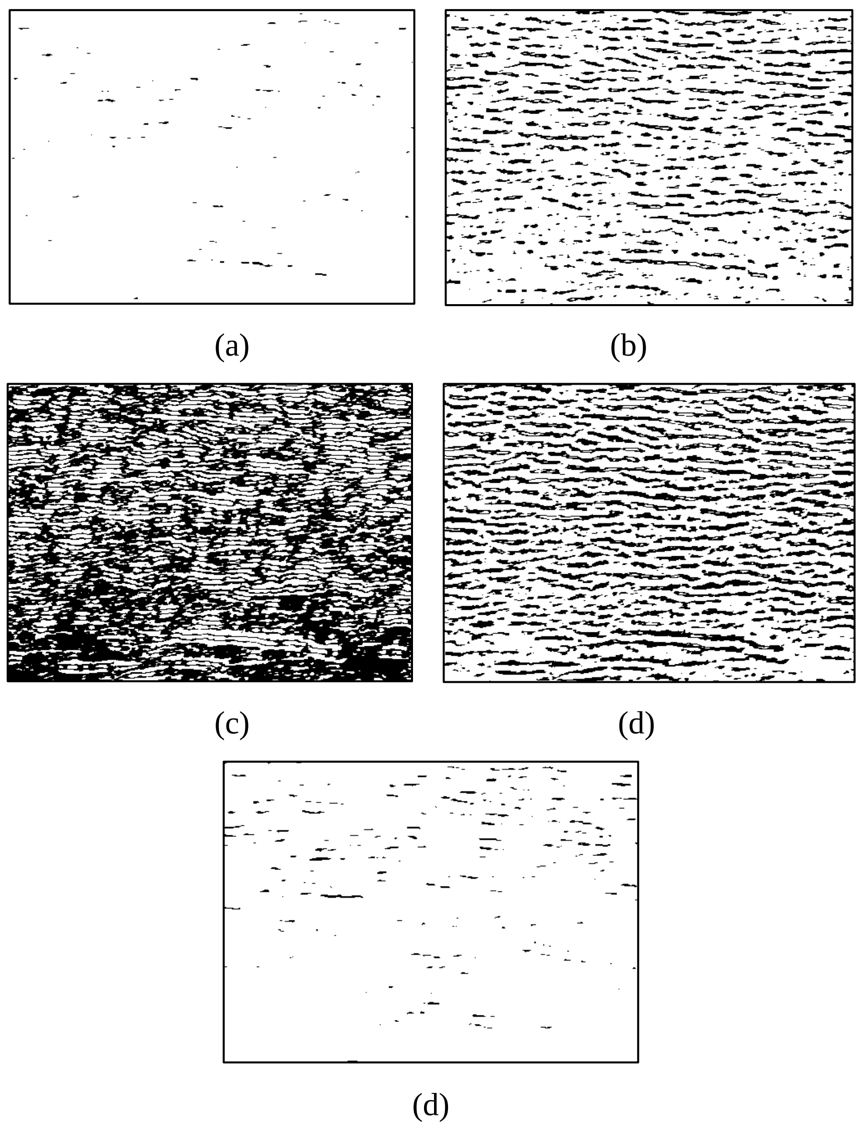

Fig. 3. Level sets for calm sea image: the decomposition of the image on nonintersecting subsets.

4.2 Density function method - Blue component of RGB

Calculation of density function values for images of calm and disturbed sea surface presented in Blue component of RGB led to the following results. The interval of density function values for calm sea is [1.9,2.09], for disturbed sea is [1.7,2.28]. We see that the first interval is rather narrow, which means that intensities of pixels change a little, and the image has more uniform structure, whereas for the disturbed sea the more complex structure is revealed. Level sets were constructed with step 0.05. Graphs of multifractal spectra for images in blue component are given on Fig. 4.

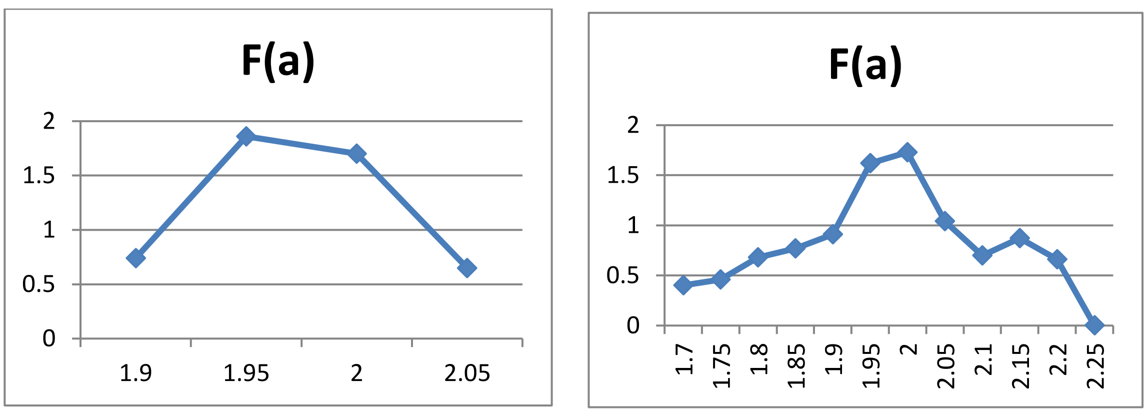

Fig. 4. Multifractal spectra for calm (left) and disturbed (right) sea surface. The images are represented in Blue component of RGB.

4.3. Method using generalized statistical sum - Grayscale

The application of the second method results in the graphs shown on Fig. 5.

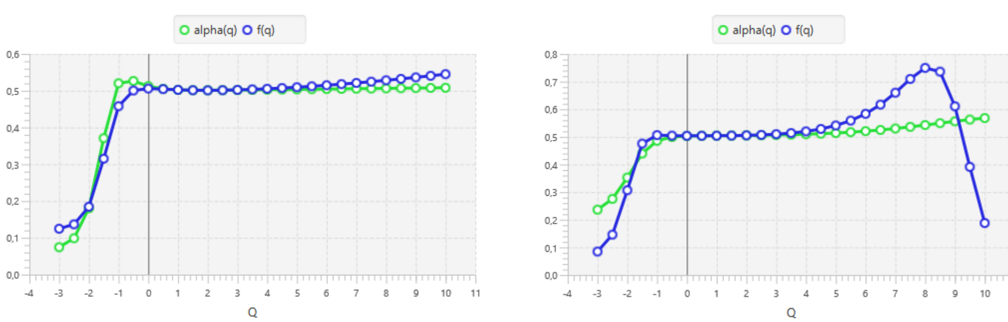

Fig. 5. Graphs of singularity and information dimensions for calm sea (left) and disturbed sea (right) in grayscale.

4.4 Method using generalized statistical sum - Blue component

We performed calculations for the representation of images in blue component. The results are shown on Fig. 6. We see that graphs are different independent of color representation.

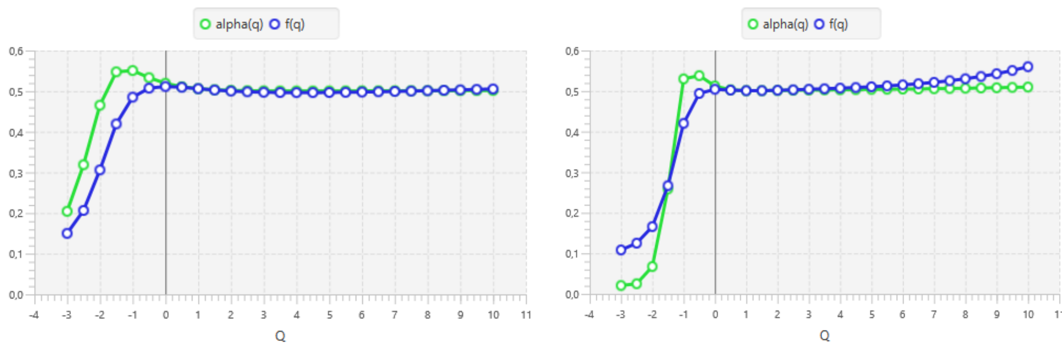

Figure 6. Graphs of singularity and information dimensions for calm sea (left) and disturbed sea (right) in Blue component.

5. CONCLUSION

The results of numerical experiments show that the methods applied may be useful for analysis of sea surface images and sea state determination, since graphs of multifractal spectra look quite different for different types of sea surfaces. It should be noted that we observe it in various color representation. The methods are rather perspective for analysis of images having complex structure such as images considered to determine sea state.

ACKNOWLEDGEMENT

Three (3) of the authors (A. Kotopoulis, G. Pouraimis and P. Frangos) would like to thank FFI Institute of Oslo, Norway, for the two (2) optical images of the sea surface, related to sea state determination (images obtained by FFI during 'NEMO 2014' trials in Taranto, Italy, September 2014). Furthermore, the authors acknowledge the support by the 'International Mobility Program', National Technical University of Athens (NTUA), Greece, which facilitated the scientific collaboration between the authors of this paper in the area of 'fractal techniques'.

REFERENCES

[1] E. Gurevich, N. Ampilova, I. Soloviev. "On a natural-science investigation of the ultralow doses effect", Proc. 8 Int. Conf. CEMA13, 17-19 Oct. 2013, Sofia, Bulgaria. p. 85-88.

[2] N. Ampilova, I. Soloviev. "Fractal analysis methods in investigation of low doses effects", Proc. 12 Int. Conf. CEMA17, 12-14 Oct. 2017, Sofia, Bulgaria, p. 10-14.

[3] N. Ampilova, E. Kulikov, V. Sergeev, I. Soloviev. "Fractal analysis methods in investigation of biomedical preparations images". Differential equations and control processes, 1, 2018, p. 109-125, http://www.math.spbu.ru/diffjournal/pdf/ampilova3.pdf (in Russian)

[4] Yong Xu, Hui Ji, Cornelia Fermuller, "Viewpoint Invariant Texture Description Using Fractal Analysis", Int. J. Comp. Vis, 2009, 83, p. 85-100.

[5] Ashvin B. Chhabra, Charles Meneveau, Roderick V. Jensen and K. R. Sreenivasan. "Direct determination of the f(α) singularities spectrum and its application to fully developed turbulence", Physical Review A, Volume 40, Number 9, November 1, 1989. p. 5284-5294.

[6] N. Ampilova, V. Sergeev, I. Soloviev. "On some questions concerning to the multi-fractal spectra calculation", Proc. 10 Int. Conf. CEMA15, 15-17 Oct. 2015, Sofia, Bulgaria. p. 14-17.

[7] N. Ampilova, I. Soloviev, J. Barth. "Application of fractal analysis methods to images obtained by crystallization modified by an additive", Journal of Measurements in Engineering, Vol. 7, Issue 2, 2019, p. 48-57. https://doi.org/10.21595jme.2019.20436.